Title

Elucidating the influence of residual polymer and gas environment on the electronic structure of a graphene layer using in situ APXPS

Authors

Yun, Dong-Jin

Etxebarria, Ane

Lee, Kyung-Jae

et al.

Publication Date

2020-10-01

DOI

10.1016/j.apsusc.2020.146764

Peer reviewed

Elucidating the influence of residual polymer and gas environment on the electronic structure of a graphene layer using in situ APXPS

Dong-Jin Yun[a,b,*], Ane Etxebarria[b,c,d], Kyung-Jae Lee[b,e], Chang Hoon Jung[a], Dong-Su Ko[a], Min-Su Seol[a], Hae-ryong Kim[a], Woo-Sung Jeon[a], Eun-ha Lee[a], JaeGwan Chung[a], Ethan J Crumlin[b,f*]

[a] Analytical Engineering Group, Samsung Advanced Institute of Technology, Suwon 440-600, South Korea

[b] Advanced Light Source, Lawrence Berkeley National Laboratory, Berkeley, CA 94720, USA

[c] Centre for Cooperative Research on Alternative Energies (CIC energiGUNE), Basque Research and Technology Alliance (BRTA), Alava Technology Park, Albert Einstein 48, 01510 Vitoria-Gasteiz, Spain

[d] Departamento de Física de la Materia Condensada, Facultad de Ciencia y Tecnología, Universidad del País Vasco, UPV/EHU, Apdo 644, 48080 Bilbao, Spain

[e] Department of Physics and Photon Science, Gwangju Institute of Science and Technology, Gwangju 500-712, South Korea

[f] Chemical Sciences Division, Lawrence Berkeley National Laboratory, Berkeley, CA 94720, USA

*Corresponding author E-mail: dongjin.yun@samsung.com & ejcrumlin@lbl.gov

1st revision submitted to Applied Surface Science

May. 10, 2020

Abstract

We use *in situ* ambient pressure X-ray photoelectron spectroscopy (APXPS) and ultraviolet photoelectron spectroscopy (UPS) to develop an effective method for studying changes in the graphene (Gr) electronic structure according to certain circumstance. The amount of polymethyl methacrylate (PMMA) residual polymer (RP), inevitably generated during the Gr transfer process, is significantly reduced from Gr surface by thermal annealing. This processed Gr is then sequentially exposed to specific gas environments (Ar, N_2, O_2, and CO_2), and APXPS or UPS is carried out to investigate the variations in the Gr electronic structure including the work function. When the amount of PMMA RP on Gr is reduced, the position of the main carbon peak shifts by more than 0.4 eV to a higher binding energy (in XPS spectra), and the secondary electron cutoff moves by about 0.2 eV to a lower binding energy (in UPS spectra). These changes are generally caused by a decrease in the Gr work function. On the other hand, exposure to the gas environments at different temperatures that we investigated did not produce significant changes in the work function and chemical states of Gr. These results confirm that the material in contact with Gr should be considered to achieve the desired Gr performance in electronics.

Keywords: Graphene, ambient pressure x-ray photoelectron spectroscopy, ultraviolet photoelectron spectroscopy, electronic structure, work function

Introduction

To overcome the limitations of conventional silicon-based electronics, research on material sciences is actively ongoing from various perspectives [1-4]. Especially in the present industry, there is a strong demand for candidate materials with better mechanical flexibility, optical transparency, chemical/thermal stability and electrical characteristics than conventional inorganic/metal materials [1-4]. Graphene (Gr), which is a single layer of a two-dimensional carbon lattice, is considered an excellent material that can meet these requirements [4-7]. Gr is typically in the form of an assembly of densely bounded sp^2-hybridized state carbon atoms. Such a unique configuration provides strong mechanical flexibility, optical transmittance (>90%), chemical/thermal stability, and charge carrier mobility (>10,000 cm^2/Vs) [4-7]. When part of a transparent conductive oxide (TCO), Gr generally provides superior characteristics to commonly used conventional TCOs such as indium tin oxide (ITO), fluorine doped tin oxide, or doped zinc oxide [4-7].

Various aspects of Gr-related materials have been studied to take advantage of their strengths in real industry. In particular, whether or not the properties of Gr vary depending on a given situation has long been a crucial consideration [5,8-10]. Even though typical material properties stay almost the same, the carrier concentration of Gr clearly differs depending on the substance in contact. Specifically, a representative example is the adsorption of electron-withdrawing or -donating dopant molecules on Gr [11,12]. When electron-withdrawing or -donating molecules are adjacent to Gr, the electron transfer from Gr to the dopant or vice versa occurs at the interfacial region. This process changes the electron concentration and work function of Gr. Thus, it is possible

to change the material properties of Gr depending on its synthesis process or operating gas environment. The following factors still need to be addressed for the primary processes used for Gr synthesis: how much the residual polymer (RP) remains on Gr or the gas surrounding Gr make an influence on the actual device operation [13-15].

Much effort has gone into the development of various analytical methodologies to examine changes in Gr chemical states and electronic structures. Among them, ultraviolet photoemission spectroscopy (UPS) and X-ray photoemission spectroscopy (XPS) are regarded as the most powerful analysis tools [12-15]. In particular, continuous developments have led to ambient pressure XPS (APXPS) and UPS analysis methods, which can now characterize Gr electronic configurations while or even after Gr is exposed to a certain environmental condition [12,16-18]. In other words, current UPS/XPS-based analytical methods allow of determining the degree of change to Gr electronic structures depending on the amount of RP adsorption or type of exposure gas. Nevertheless, to the best of our knowledge, there have been rarely reported on the characterization of Gr electronic structure in real gas environment using APXPS method.

In this study, we prepared a Gr layer on a SiO_2 substrate (Gr/SiO_2) by chemical vapor deposition (CVD) and wet transfer processes [6,19,20]. Then, the changes to the electronic structure according to certain environmental conditions were examined with two different photoemission spectroscopy (PES) methods: synchrotron-beam based APXPS and He-II source-based UPS. The analyses were performed before and after thermal annealing and gas exposure. Our results clearly elucidated how changes in the RP amount and gas environment influence the energy level alignments of the Gr/SiO_2

structure, which we used to determine which is more influential on the Gr electronic structure.

Materials and methods

A highly crystalline Gr layer was grown on copper foil through CVD and then transferred to a 6-in (300 nm) SiO_2/Si wafer by the wet-transfer method with a polymethyl methacrylate (PMMA) stamp. The detailed information about the Gr growth/transfer processes is given elsewhere [6,7,19,20]. During these processes, a considerable amount of PMMA RP with a small dose of the metal etchant ($FeCl_3$) unavoidably remained on the Gr surface.

The PES methods are primarily used to investigate changes in Gr chemical state and electronic structures depending on the circumstances and are divided into two major categories: *in situ* APXPS and *in situ* UPS. For the APXPS analysis, the Gr-coated SiO_2/Si wafer (i.e., the Gr/SiO_2 structure) was cut to have an area of about 1 × 1 cm^2. Then, it was loaded into the equipment of the Advanced Light Source (ALS) Beamline 9.3.2, as shown in Figure 1. The ALS Beamline 9.3.2 is equipped with a bending magnet and two grating monochromators of 100 lines (l)/mm and 600 l/mm. Thus, the incident photon energy (hυ) can be adjusted within the energy range of 200–800 eV. Meanwhile, the electron analyzer (Scienta R4000 HiPP) was set to a pass energy of 100 eV, step of 100 meV, and dwell time of 200 ms. These settings provided a total resolution (source and analyzer) of about 220 meV at room temperature (RT) for the given photon energies.

As a first step, the chemical/electronic configurations of Gr/SiO_2 structures were investigated in an Ar gas environment at 400 mTorr with different temperatures. In other

words, the XPS spectra of the Gr/SiO_2 structure were obtained as the temperature was increased from RT to 250 °C and then 500 °C before being cooled down back to RT. Meanwhile, the Ar gas pressure was maintained at 400 mTorr. The Gr/SiO_2 structure was then measured with XPS at different annealing temperatures in a certain gas environment, where N_2, O_2, or CO_2 gas at 400 mTorr was added to Ar gas at 400 mTorr. For each condition, the XPS measurement was performed at two photon energies (430 or 500 eV) to enhance the experimental reliability. There is a possibility of charging due to defective, dangling, trap sites or impurity/contamination at interface region. So, depending on the photon energies, the electrons emitted from the Gr components in Gr/SiO_2 structure are able to be emitted from Gr/SiO_2 structure have slight binding energy differences [21-23].

In situ UPS was used to analyze any obvious changes in the Gr electronic structure after exposure to different gas environments. UPS was performed with a He II (hν: 40.8 eV) photon source at an applied voltage of 5 V. UPS measurements requiring an ultrahigh vacuum (UHV) condition of over 10^{-8} Torr proceeded after the sample was exposed to a certain gas environment. An as-prepared sample of the Gr/SiO_2 structure was loaded into the UHV chamber at ~10^{-9} Torr. Then, the UPS spectra were obtained as the annealing temperature was increased from RT to 400 °C. The sample was exposed to a N_2 gas environment at 400 mTorr for 2 h immediately after being cooled down to RT. Next, the temperature of the sample was increased to 200 and 400 °C when in the N_2 gas environment. This process lastly repeated under O_2 gas environment. UPS was used for measurements after each stage.

The sheet resistances of the Gr layers were measured with a four-point probe. Optical microscopy images and Raman mapping images with spectra were characterized

with Micro-Raman_S (inVia, 514.54 nm). Atomic force microscopy (AFM) was carried out with Bruker's FastScan. High-resolution transmission electron microscopy (HRTEM) was then performed by using a FEI Titan3 G2 60-300 equipped with double aberration correctors (image and probe) and monochromator at a low acceleration voltage of 80 kV.

Results and discussion

The schematic diagram in Figure 1 shows how the sample of the Gr/SiO_2 structure was loaded and each experimental step of the APXPS measurement in the ALS Beamline 9.3.2. In contrast to conventional XPS equipment in a laboratory, this beamline allows XPS measurements in a certain gas environment at several hundred torr [17,18,24]. In addition to the basic chemical configuration, changes in the XPS spectra provided information on the surface chemical reaction with specific gas molecules and the energy alignment at the solid–gas interface. In other words, the growth or reduction of chemical states in the XPS core-level spectra corresponded to changes in the chemical bonds, while the binding energy shift between the chemical states of different substances was associated with the surface potential at the interface [24,25]. Accordingly, the peak positions in the XPS spectra obtained in different gas environments were used as a criterion for characterizing the transition behavior of Gr chemical states and electronic structures [18,25,26]. With respect to the Si–O_x peak position, a shift of the carbon main peak to a higher binding energy indicated n-type doping of Gr, while a shift to a lower binding energy indicated p-type doping [13,20,27].

We investigated the Ar gas core-level structure in each gas environment at different annealing temperatures. The resulting XPS spectra were used to measure changes in the doping state of Gr. Depending on the sample work function, the vacuum level (VL) of a gas changed, but the ionization potential (IP) remained constant [28,29]. Therefore, the binding energy of Ar gas indicated relative changes in the sample work function when experimental conditions such as the partial gas pressure, distance from the electron analyzer, and gas composition were fixed [28, 29].

Using the PMMA-based wet-transfer process to place a Gr layer on a SiO_2 substrate unavoidably left varying degrees of PMMA RP on the surface [5-7]. The RP clearly influenced the material properties of Gr; it generally degraded the uniformity of the morphology (roughness) and optical properties (transmittance and haze) of Gr and completely changed the electronic properties. The HRTEM image in Figure S1 clearly shows how the PMMA RP adsorbed on the honeycomb lattice structure of Gr. On top of this surface, RP chunks with various sizes from the sub-nanometer scale to tens of nanometers stuck strongly depending on the location.

Thermal annealing in an Ar environment at 400 mTorr was used to remove the PMMA RP from the Gr surface. The APXPS core-level spectra of Gr sample were obtained at different temperatures during the annealing process. These results elucidated the changes in the Gr electronic/chemical structure with decreasing RP. We believe that the removal of PMMA RP can be used to measure the restoration of the original characteristics of Gr. Fig. 2 shows XPS spectra that were obtained for a certain thermal annealing process: (a, b) C 1*s*, (d, e) Ar 2*p*, and (g, h) Si 2*p*). During the XPS measurement, unexpected changes in the gas pressure may shift the peak positions in

XPS core-level spectra. For this reason, we tried to keep the Ar gas pressure at 400 mTorr, and the XPS measurement was carried out at two photon energies of 430 and 500 eV. The Si–O_x chemical state of the SiO_2 substrate, which appeared at ~103.6 eV in the Si 2*p* core level, was used as a criterion for calibrating the peak position. The Gr layer mainly consisted of C–C and C=C bonds, and its chemical state was located at about 283.8±0.1 eV (hυ 430 eV:283.76 eV and hυ: 500 eV:283.87 eV) before the thermal annealing process. The chemical state of the Ar gas phase was also observed in the Ar $2p_{3/2}$ core-level structure (hυ 430 eV:243.44 eV and hυ 500 eV:243.23 eV). The intensity of Ar 2p spectra gradually decreases with increasing temperature because the Ar gas density near sample is proportional to the pressure/temperature ratio of the ideal gas law [30]. Their shifts in the peak position during or after thermal annealing process allowed us to identify changes in the Gr electronic structure. As the annealing temperature increased, the peak positions of the C–C and C=C bonds gradually moved to higher binding energies for each C 1*s* core-level structure obtained with different photon energies (hυ 430 eV: from 283.76 eV to 284.38 eV and hυ 500 eV: 283.87 eV to 284.30 eV). The same changes in behavior were observed at the Ar 2*p* core levels; the peak of the Si–O_x chemical state remained unchanged at a binding energy of about 103.6 eV. Figures 2(c), (f), and (i) summarize the peak shifts described above. The shifts in the peak positions of the C–C and C=C bonds or Ar gas phase to a higher binding energy were most likely due to the obvious decrease of PMMA RP on Gr, considering that they remained even after the temperature was lowered to RT. This interpretation was clearly supported by the results of the AFM, UPS, and Raman analyses.

After thermal annealing at 400 °C under the UHV condition, several nanoscale lumps on the Gr surface noticeably disappeared, as shown in AFM images of Figure S2 (a)-(c) (root mean square of as-deposited Gr: 0.992 nm; root mean square of annealed Gr: 0.711 nm). The changes in the UPS spectra of Gr/SiO_2 according to the annealing temperature can be a good criterion for investigating the PMMA adsorbed on Gr. The PMMA RP on Gr is known to act as a p-type electron-withdrawing dopant [31,32]. Therefore, if the amount of PMMA RP on Gr is decreased by thermal annealing, this could reduce the work function of Gr. The work function was calculated from the UPS spectra as follows [1,12]:

$$\Phi = h\nu\ (\text{He II} = 40.8\ \text{eV}) - E_{Cutoff} + E_{Fermi} \quad (1)$$

where Φ, $h\upsilon$, E_{cutoff}, and E_{Fermi} correspond to the work function of Gr, the incoming photon energy of 40.8 eV from the He II source, the secondary cutoff energy in the UPS spectra, and the Fermi energy (binding energy of 0 in UPS spectra), respectively. Both the UPS spectra and calculated work function are displayed in Figures S3(a)–(c). As the annealing temperature increased, the Gr work function gradually decreased from about 4.68±0.02 eV to 4.47±0.03 eV. As the annealing temperature increased, the electronic structure in the valence band became more like that of Gr, while the chemical states of PMMA RP obviously disappeared [33,34]. The UPS results elucidate that removing PMMA RP from the Gr layer led to the n-type doping effect on the Gr electronic structure. Similarly, the Raman results clearly support n-type doping effects on Gr due to thermal annealing under the UHV condition. The peak position of the G band shifted by a wavenumber of about 4 and such shift to a lower wavenumber corresponds to n-type doping of Gr.

As discussed previously, a large amount of PMMA RP was removed from the Gr layer by thermal annealing. To study the reactivity of Gr to specific gases, this sample was then immediately placed into different gas environments without being exposed to air. N_2 gas at 400 mTorr was added to the Ar gas at 400 mTorr; then, the XPS spectra of the Gr/SiO_2 structure were obtained at different temperatures (RT, 250 °C, and 500 °C) at a total gas pressure of 800 mTorr. Similarly, the experiments in O_2 and CO_2 gas environments were performed in sequence (see Figure 1). The XPS results for the exposure to each gas environment (N_2 + Ar, O_2 + Ar, and CO_2 + Ar mixed gas) are displayed in Figures 3 and S5–S7). Because there was little difference in the analysis depth between the photon sources at 430 and 500 eV, the XPS results with those two different sources were assumed to show similar transition behaviors according to the environment. Thus, their common trend changes were considered as the standard for judging the Gr electronic structure at a specific analysis stage. For the C 1*s* core-level structures in Figures 3(a)–(i), there were no obvious changes in the peak positions of the C–C and C=C bonds depending on the gas environment. Their variations were less than 0.1 eV, and the transition behavior showed no obvious consistency. The XPS spectra indicated no further growth of the C–O bond in the Gr layer despite exposure to reactive O_2 or CO_2 gas. On the other hand, the binding energy of Ar gas in a mixed state with other gases does not give a clear change behavior because it also varies depending on variables other than the sample work function, such as the mixing ratio of gases near the sample surface and the interaction between the two gases. So, although Ar gas was included in all gas environments, it was not possible to use it for calculating the work function without a delicate calibration process. In summary, the XPS results indicated

that the different gas environments had little effect on the Gr electronic structure, including the work function and doping state. This is in contrast to the effect of reducing the amount of PMMA RP on the Gr surface.

The UPS measurement was conducted for each gas exposure and thermal annealing process in homemade PES equipment (See Figure S8) as another way to analyze the gas environment effects on the Gr properties. Unlike APXPS, UPS cannot be performed in an actual gas environment; thus, this experiment provided information about whether Gr showed obvious changes in the electronic structure before and after exposure to a specific gas environment. To reduce the PMMA RP on the Gr surface, the sample of the Gr/SiO_2 structure was subjected to thermal annealing at 400 °C. This eliminated the chemical states related to PMMA RP, which decreased the work function of Gr. Such changes due to thermal annealing in an Ar environment (see Figures S9(a) and (b)) are mostly similar to those from thermal annealing in UHV (see Figures S3(a) and (b)). On the other hand, the Gr electronic structure has few changes even after exposure to a N_2 or O_2 gas environment at different temperatures, and stay it similar to that obtained from clean Gr [35]. The experimental sequence shown in Figure 4(b) was employed, and UPS measurements were performed between stages of specific gas environments in steps 1–8. As shown in Figures 4(c) and (d), there is the slight changes in electronic configuration due to the carbon contamination adsorption at R.T., however, the valence band still retains its structure similar to that of clean graphene. Accordingly the secondary electron cutoffs in the actual UPS spectra stayed almost the same after exposure to each gas condition.

Figure 5 sums up the results of the APXPS and *in situ* UPS analyses and describes the change trend of the Gr electronic structure according to the amount of PMMA RP on Gr or gas exposure condition. When a considerable amount of PMMA RP is removed by thermal annealing, the work function of Gr decreases because of the n-type doping effect. The UPS results directly reflected the decrease in the Gr work function with the transition of the valence band. Such changes are directly connected with the shift of the carbon main peak to a higher binding energy in the APXPS results. In contrast, exposing the Gr electronic structure to different gas environments had an insignificant impact. Although the reactive gases of N_2, O_2, and CO_2 were injected close to the limit, there was no obvious transition in both the carbon main peak and secondary electron cutoff for all tested gas environments. The Gr electronic structure remained almost the same during (APXPS: pN_2, pO_2 and pCO_2 of 400 mTorr) or after (*in situ* UPS: pN_2 and pO_2 of 400 mTorr) exposure to a specific gas environment.

Conclusions

We used PES-based methods to develop an effective approach to characterizing the changes to the Gr electronic structure according to the situation. We controlled the amount of PMMA RP on Gr and the gas environment to investigate changes in the peak positions of the main carbon bonds and secondary electron cutoff position for the valence band shape with APXPS and *in situ* UPS. We compared the results of these methods to measure changes in the Gr work function with different PMMA RP amounts and gas environments, including the annealing temperature. The results confirmed that the Gr electronic structure is more strongly influenced by the amount of PMMA RP than by the

gas environment. The findings of this study show that the material in contact with Gr is an essential consideration for achieving excellent performance with Gr-based electronics.

Acknowledgments

The research used resources of the Advanced Light Source, which is a DOE Office of Science User Facility under contract no. DE-AC02-05CH11231. A.E. thanks the Basque Government for funding through a PhD Fellowship (Grant no. PRE_2018_2_0285) and through Egonlabur Travel Fellowship (Grant no. EP_2018_1_0004). E.J.C. was partially supported by an Early Career Award in the Condensed Phase and Interfacial Molecular Science Program, in the Chemical Sciences Geosciences and Biosciences Division of the Office of Basic Energy Sciences of the U.S. Department of Energy under Contract No. DE-AC02-05CH11231.

References

[1] S. W. Rhee, D. J. Yun, Metal-semiconductor contact in organic thin film transistors, J. Mater. Chem. 18 (2008) 5437-5444.

[2] Y. Wang, L. Sun, C. Wang, F. Yang, X. Ren, X. Zhang, X. Zhang, H. Dong, W. Hu, Organic crystalline materials in flexible electronics, Chem. Soc. Rev. 48 (2019) 1492-1530.

[3] S. E. Root, S. Savagatrup, A. D. Printz, D. Rodriquez, D. J. Lipomi, Mechanical properties of organic semiconductors for stretchable, highly flexible, and mechanically robust electronics Chem. Rev. 117 (2017) 6467-6499.

[4] L. Yu, C. Shearer, J. Shapter, Recent development of carbon nanotube transparent conductive films, Chem. Rev. 116 (2016) 13413-13453.

[5] M. J. Allen, V. C. Tung, R. B. Kaner, Honeycomb carbon: a review of graphene Chem. Rev. 110 (2010) 132-145.

[6] S. Bae, H. Kim, Y. Lee, X. Xu, J. S. Park, Y. Zheng, J. Balakrishnan, T. Lei, H. R. Kim, Y. I. Song, Y. J. Kim, K. S. Kim, B. Ozyilmaz, J. H. Ahn, B. H. Hong, S. Iijima, Roll-to-roll production of 30-inch graphene films for transparent electrodes, Nat. Nanotech. 20 (2010) 1-5.

[7] K. S. Kim, Y. Zhao, H. Jang, S. Y. Lee, J. M. Lim, K. S. Kim, J. H. Ahn, P. Kim, J. Y. Choi, B. H. Hong, Large-scale pattern growth of graphene films for stretchable transparent electrodes, Nature 457 (2009) 706-710.

[8] A. D. Smith, K. Elgammal, X. Fan, M. C. Lemme, A. Delin, M. Rasander, L. Berggvist, S. Schroder, A. C. Fischer, F. Niklaus, M. Ostling, Graphene-based CO_2 sensing and its crosssensitivity with humidity, RSC adv. 7 (2017) 22329-22339.

[9] V. Panchal, C. E. Giusca, A. Lartsev, N. A. Martin, N. Cassidy, R. L. Myers-Ward, D. K. Gaskill, O. Kazakova, Atmospheric doping effects in epitaxial graphene: correlation of local and global electrical studies, 2D Mater. 3 (2016) 015006.

[10] C. Melios, A. Centeno, A. Zurutuza, V. Panchal, C. E. Giusca, S. Spencer, S. R. P. Silva, O. Kazakova, Effects of humidity on the electronic properties of graphene prepared by chemical vapour deposition, Carbon 103 (2016) 273-280.

[11] H. Liu, Y. Liu, D. Zhu, Chemical doping of graphene, J. Mater. Chem. 21 (2011) 3335-3345.

[12] D. J. Yun, S. Kim, C. Jung, C. S. Lee, H. Sohn, J. Y. Won, Y. S. Kim, J. Chung, S. Heo, S. H. Kim, M. Seol, W. H. Shin, Direct characterization of graphene doping state by in situ photoemission spectroscopy with Ar gas cluster ion beam sputtering, Phys. Chem. Chem. Phys. 20 (2018) 615-622.

[13] R. Blume, D. Rosenthal, J. P. Tessonnier, H. Li, A. Knop-Gericke, R. Schlogl, Characterizing graphitic carbon with x-ray photoelectron spectroscopy: a step-by-step approach, Chem. Cat. Chem. 7 (2015) 2871-2881.

[14] J. –K. Chang, C. –C, Hsu, S. –Y. Liu, C, -I, Wu, M. Gharib, N. –C, Yeh, Spectroscopic studies of the physical origin of environmental aging effects on doped graphene, J. Appl. Phys. 119 (2016) 235301.

[15] C. Melios, C. E. Giusca, V. Panchal, O. Kazakova, Water on graphene: review of recent progress, 2D Mater. 5 (2018) 022001.

[16] K. A. Stoerzinger, W. T. Hong, E. J. Crumlin, H. Bluhm, Y. S. Horn, Insights into electrochemical reactions from ambient pressure photoelectron spectroscopy, Acc. Chem. Res. 48 (2015)2976-2983.

[17] H. Bluhm, K. Andersson, T. Araki, K. Benzerara, C. E. Brown, J. J. Dynes, S. Ghosal, M. K. Gilles, H. –Ch. Hansen, J. C. Hemminger, A. P. Hitchcock, G. Ketteler, A. L. D. Kilcoyne, E. Kneedler, J. R. Lawrence, G. G. Leppard, J. Majzlam, B. S. Mun, S. C. B. Myneni, A. Nilsson, H. Ogasawara, D. F. Ogletree, K. Pecher, M. Salmeron, D. K. Shuh, B. Tonner, T. Tyliszczak, T. Warwick, T. H. Yun, Soft X-ray microscopy and spectroscopy at the molecular environmental science beamline at the Advanced Light Source, J. Electron. Spectrosc. 150 (2006) 86-104.

[18] S. Axnanda, E. J. Crumlin, B. Mao, S. Rani, R. Chang, P. G. Karlsson, M. O. M. Edwards, M. Lundqvist, R. Moberg, P. Ross, Z. Hussain, Z. Liu, Using "Tender" x-ray ambient pressure x-ray Photoelectron spectroscopy as a direct probe of solid-liquid interface, Sci. Rep. 5 (2015) 09788.

[19] J. Lee, Y. Kim, H. –J. Shin, C. S. Lee, D. Lee, C. –Y. Moon, J. Lim, S. C. Jun, Clean transfer of graphene and its effect on contact resistance, App. Phys. Lett. 103 (2013) 103104.

[20] J. W. Suk, W. H. Lee, J. Lee, H. Chou, R. D. Piner, Y. Hao, D. Akinwande, R. S. Ruoff, Enhancement of the electrical properties of graphene grown by chemical vapor deposition via controlling the effects of polymer residue, Nano Lett. 13 (2013) 1462-1467.

[21] X. F. Fan, W. T. Zheng, V. Chihaia, Z. X. Shen, J. L. Kuo, Interaction between graphene and the surface of SiO_2, J. Phys.: Condens. Matter. 24 (2012) 305004.

[22] S. Kobayashi, Y. Anno, K. Takei, T. Arie, S. Akita, Photoresponse of graphene field-effect-transistor with n-type Si depletion layer gate, Sci. Rep. 8 (2018) 4811.

[23] L. G. Bulusheva, V. E. Arkhipov, K. M, Popov, V. I. Sysoev, A. A. Makarova, A. V. Okotrub, Electronic structure of nitrogen- and phosphorus-doped graphenes grown by chemical vapor deposition method, Materials 13 (2020) 1173.

[24] M. E. Grass, P. G. Karlsson, F. Aksoy, M. Lundqvist, B. Wannberg, B. S. Mun, Z. Hussain, Z. Liu, New ambient pressure photoemission endstation at Advanced Light Source beamline 9.3.2, Rev. Sci. Instrum. 81 (2010) 053106.

[25] M. A. Brown, Z. Abbas, A. Kleibert, R. G. Green, Goel A, May S and T. M. Squires, Determination of surface potential and electrical double-layer structure at the aqueous electrolyte-nanoparticle interface, Phys. Rev. X 6 (2016) 011007.

[26] S. McDonnell, A. Azcatl, R. Addou, C. Gong, C. Battaglia, S. Chuang, K. Cho, A. Javey, R. M. Wallace, Hole contacts on transition metal dichalcogenides: interface chemistry and band alignments, ACS Nano 8 (2014) 6265-6272.

[27] A, Dahal, R. Addou, H. Coy-Diaz, J. Lallo, M. Batzill, Charge doping of graphene in metal/graphene/dielectric sandwich structures evaluated by C-1s core level photoemission spectroscopy, APL Mater. 1 (2013) 042107.

[28] S. Axnanda, M. Scheele, E. Crumlin, B. Mao, R. Chang, S. Rani, M. Faiz, S. Wang, P. Alivistos, Z. Liu, Direct work function measurement by gas phase photoelectron spectroscopy and its application on PbS nanoparticles, Nano Lett. 13 (2013) 6176-6182.

[29] J. Kim, W. H. Park, W. H. Doh, S. W. Lee, M. C. Noh, J. J. Gallet, F. Bournel, H. Kondoh, K. Mase, Y. Jung, B. S. Mun, J. Y. Park, Adsorbate-driven reactive interfacial Pt-NiO_{1-x} nanostructure formation on the $Pt_3Ni(111)$ alloy surface, Sci. Adv. 4 (2018) eaat3151.

[30] F. Tao, L. Nguyen, Interactions of gaseous molecules with X-ray photons and photoelectrons in AP-XPS study of solid surface in gas phase, Phys. Chem. Chem. Phys. 20 (2018) 9812-9823.

[31] A. Pirkle, J. Chan, A. Venugopal, D. Hinojos, C. W. Magnuson, S. McDonnell, L. Colombo, E. M. Vogel, R. S. Ruoff, R. M. Wallace, The effect of chemical residues on the physical and electrical properties of chemical vapor deposited graphene transferred to SiO_2, Appl. Phys. Lett. 99 (2011) 122108.

[32] W. Choi, M. A. Shehzad, S. Park, Y. Seo, Influence of removing PMMA residues on surface of CVD graphene using a contact-mode atomic force microscope, RSC Adv. 7 (2017) 6943-6949.

[33] Z. Luo, S. Lim, Z. Tian, J. Shang, L. Lai, B. MacDonald, C. Fu, Z. Shen, T. Yu, J. Lin, Pyridinic N doped graphene: synthesis, electronic structure, and electrocatalytic property, J. Mater. Chem. 21 (2011) 8038-8044.

[34] M. Salim, J. Hurst, M. Montgomery, N. Tolman, H. Liu, Airborne contamination of graphite as analyzed by ultra-violet photoelectron spectroscopy, J. Electron. Spectrosc. 235 (2019) 8-15.

[35] W. H. Lin, T. H. Chen, J. K. Chang, J. Taur, Y. Y. Lo, W. L. Lee, C. S. Chang, W. B. Su, C. I. Wu, A direct and polymer-free method for transferring graphene grown by chemical vapor deposition to any substrate, ACS Nano 8 (2014) 1784.

Figure captions

Figure 1 The schematic diagram elucidating how the sample of Gr/SiO2 structure was loaded and each of experimental steps was gone through in 9.3.2 beamline in ALS for APXPS measurement.

Figure 2 The XPS spectra of Gr/SiO_2 structure obtained under Ar gas environment at different temperatures. Each of XPS core levels were investigated with two photon energies of 430 eV ((a) C 1s, (d) Ar 2p and (g) Si 2p) and 500 eV ((b) C 1s, (e) Ar 2p and (h) Si 2p) to enhance experimental reliability and based on these results, the centers of C-C/C=C peak (c), Ar $2p_{3/2}$ peak (d) and Si-O_x peak (e) were summarized as a result.

Figure 3 The C 1s core levels of Gr/SiO_2 structures measured under different gas environments: 1) N_2 gas (400 mTorr) with Ar gas (400mTorr) - (a) hv: 430 eV, (b) hv: 500 eV and (c) the center-positions of C-C/C=C peaks obtained, 2) O_2 gas (400 mTorr) with Ar gas (400mTorr) - (d) hv: 430 eV, (e) hv: 500 eV and (f) the center-positions of C-C/C=C peaks obtained and 3) CO_2 gas (400 mTorr) with Ar gas (400mTorr) - (g) hv: 430 eV, (h) hv: 500 eV and (i) the center-positions of C-C/C=C peaks obtained.

Figure 4 Whole experimental sequence used to carry out the UPS measurement after exposing to specific gas environment at different annealing temperatures. The resulting UPS spectra, consisting of secondary cutoff and valence band regions, obtained after exposing each of gas conditions.

Figure 5 The summary of APXPS and *in-situ* UPS results, which describes the change trend of the Gr electronic structure according to the amount of PMMA RP on Gr or gas exposure conditions.

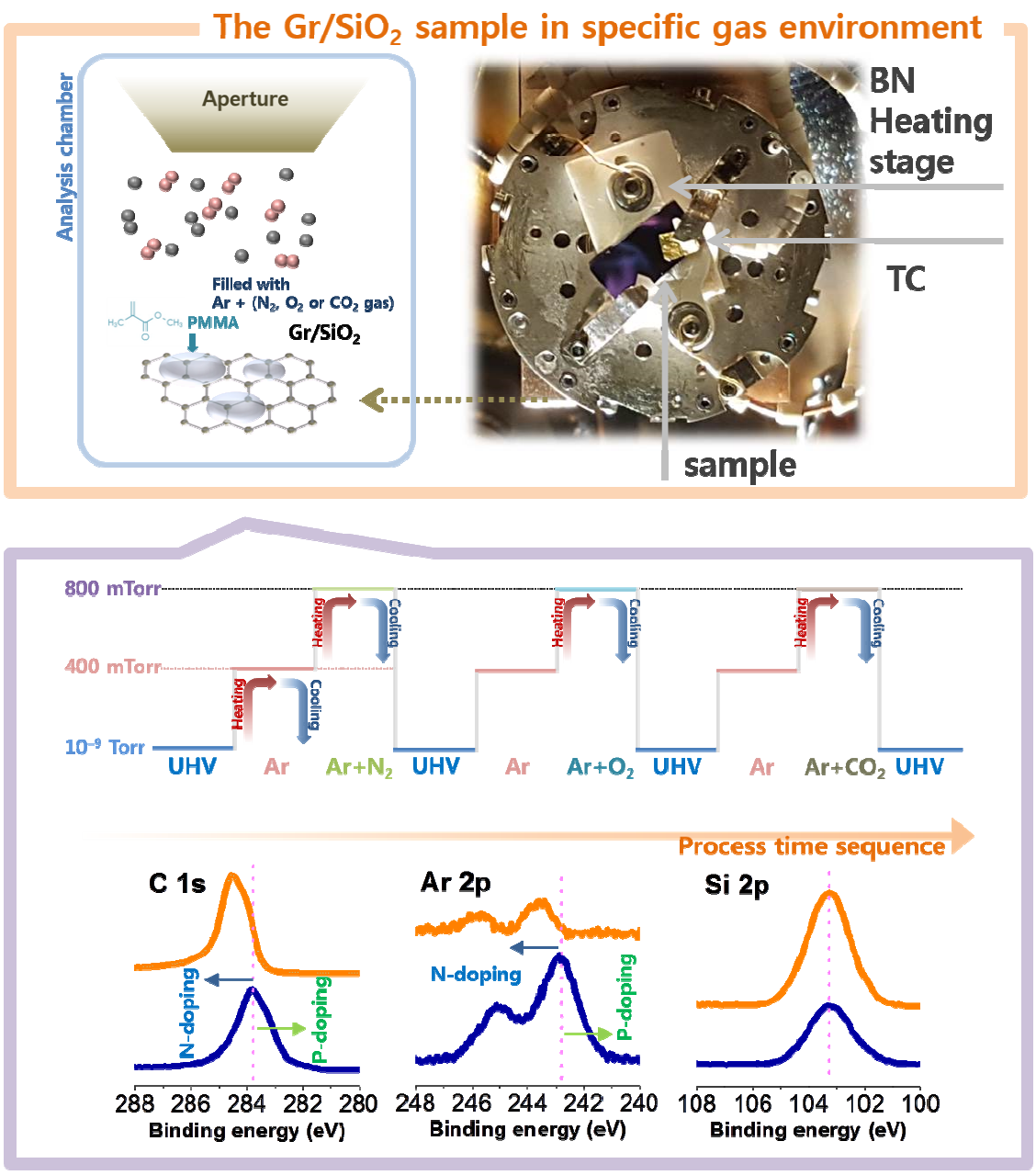

Figure 1. Yun et al.

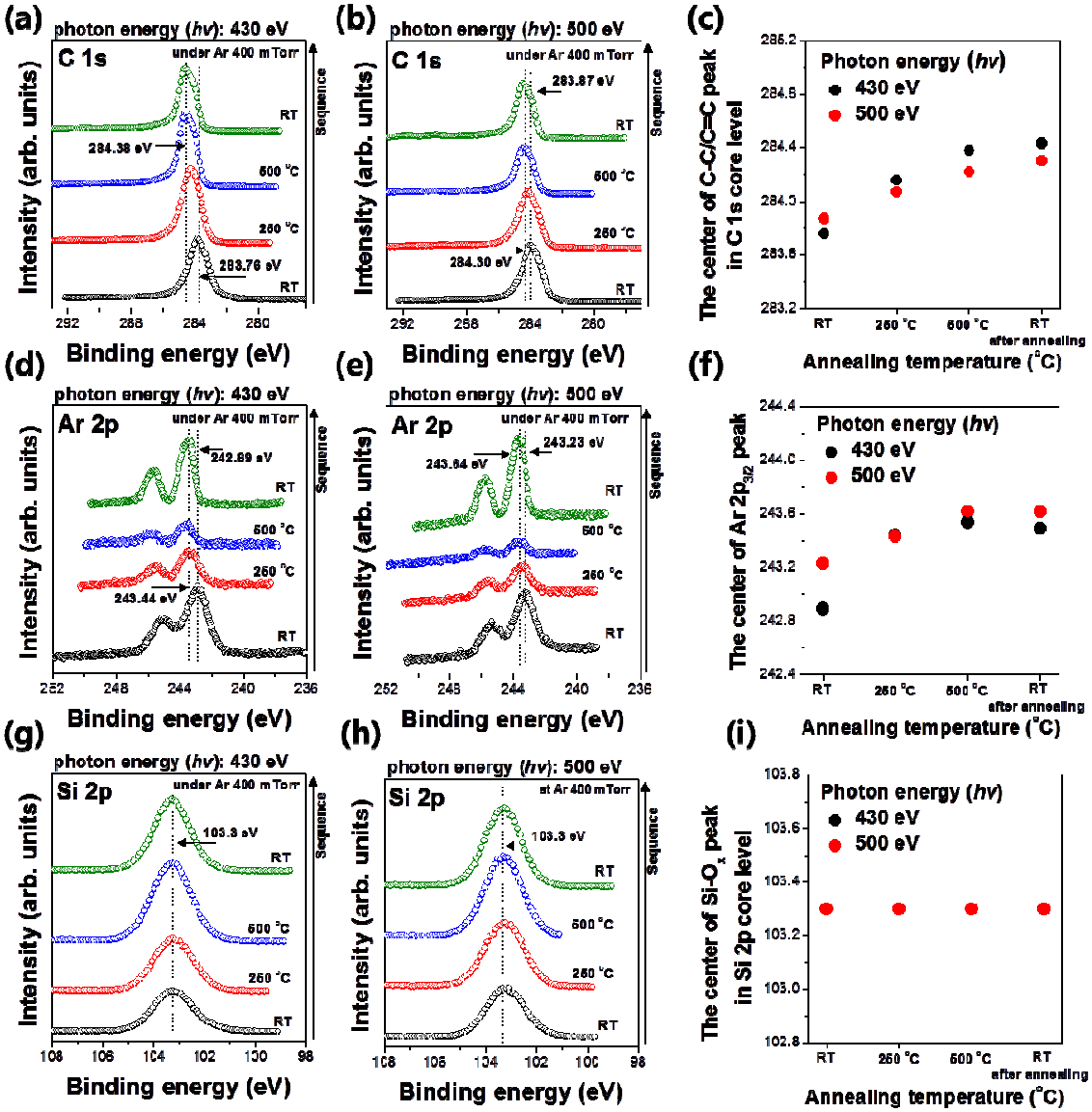

Figure 2. Yun et al.

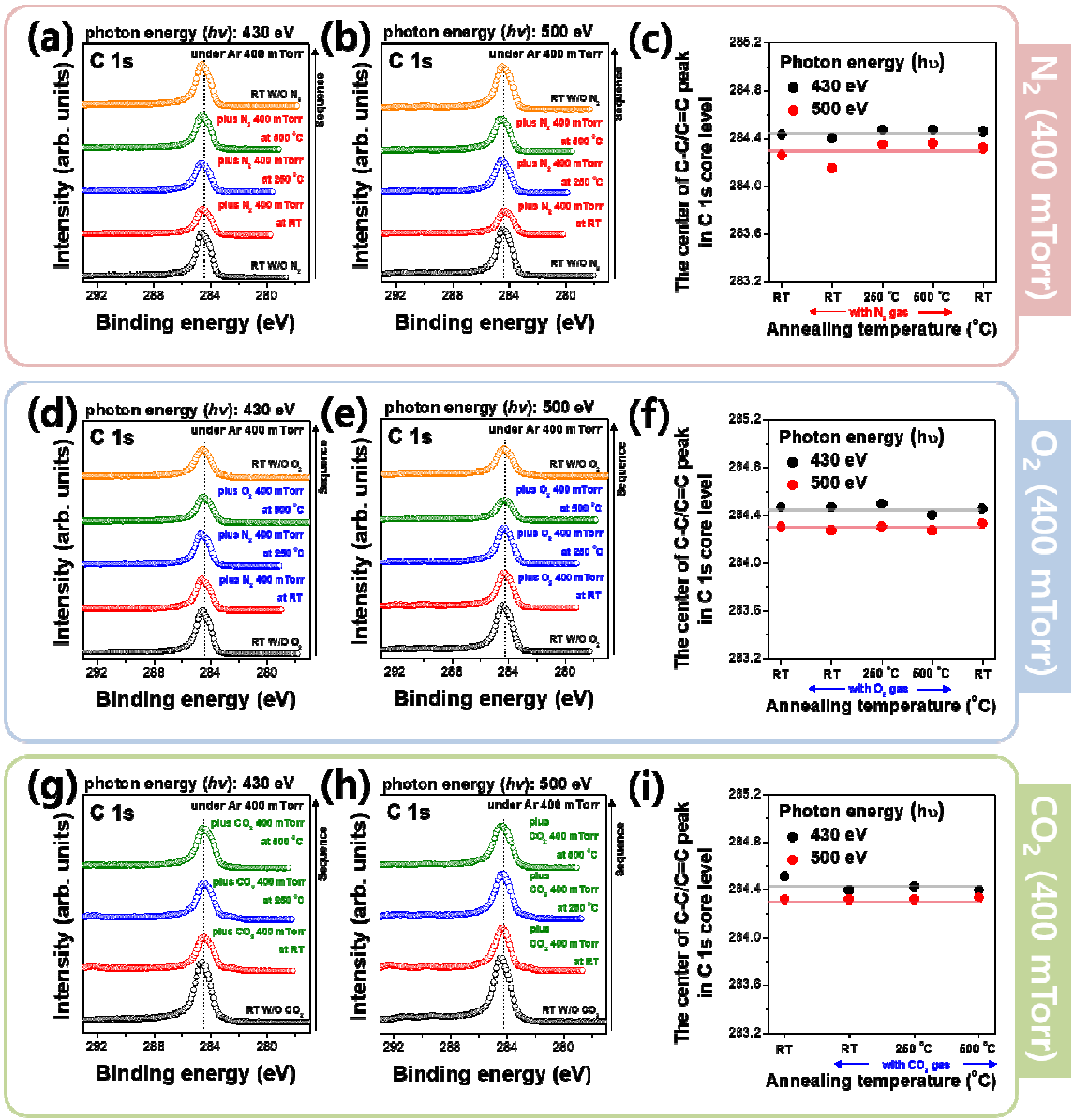

Figure 3. Yun et al.

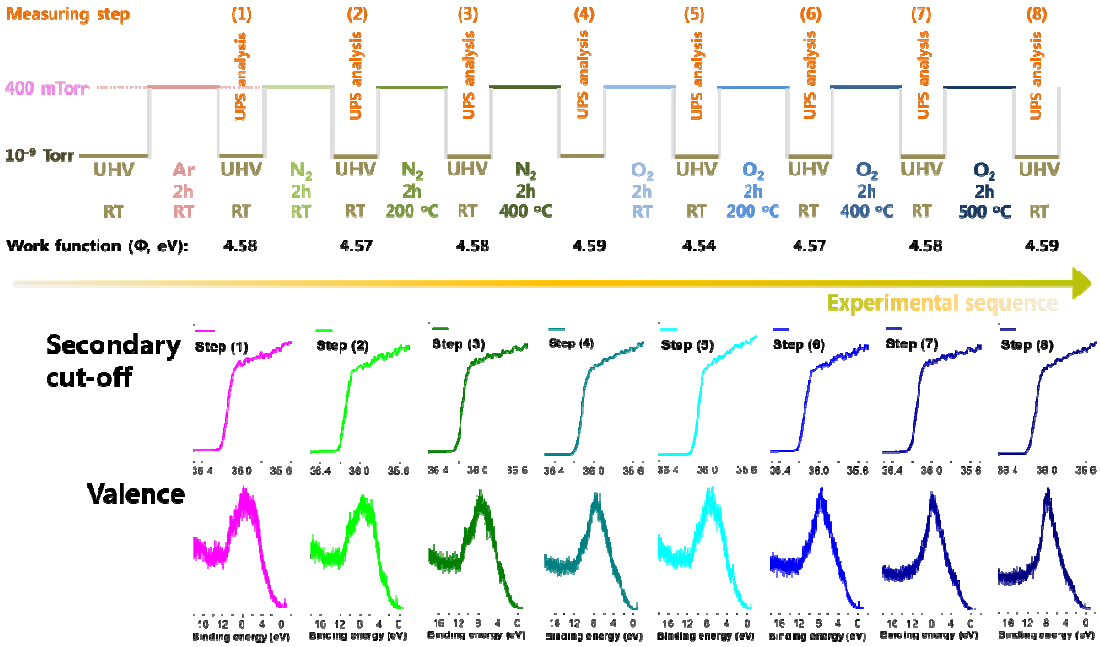

Figure 4. Yun et al.

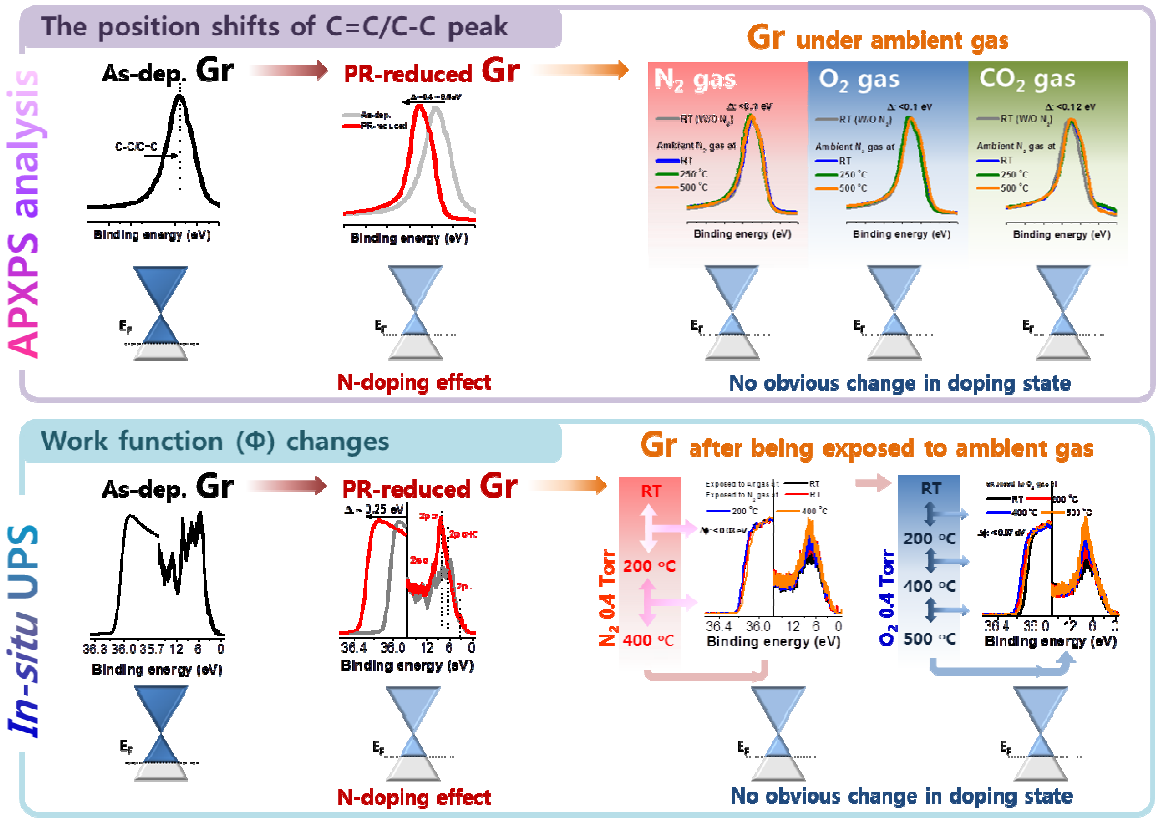

Figure 5. Yun et al.

ALS
ADVANCED LIGHT SOURCE

APXPS analysis: Characterization of Gr electronic structure in real gas environment

9.3.2 beamline

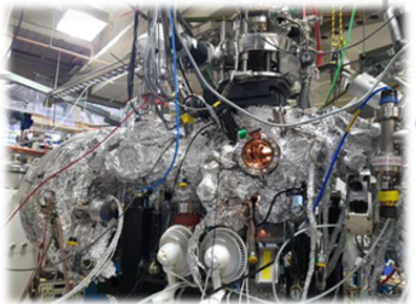

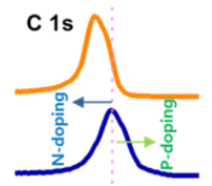

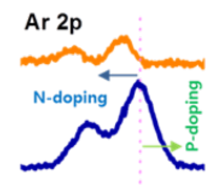

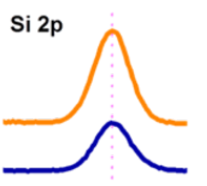

The work function of Gr